THE JOURNAL OF BIOLOGICAL CHEMISTRY VOL. 286, NO. 33, pp. 29292–29302, August 19, 2011

Ligand Modulation of the Epstein-Barr Virus-induced Seven-transmembrane Receptor EBI2

IDENTIFICATION OF A POTENT AND EFFICACIOUS INVERSE AGONIST[S]

Received for publication, October 20, 2010, and in revised form, June 10, 2011 Published, JBC Papers in Press, June 14, 2011, DOI 10.1074/jbc.M110.196345

Tau Benned-Jensen[‡], Christopher Smethurst[§], Peter J. Holst[¶], Kevin R. Page[§], Howard Sauls[‖], Bjørn Sivertsen[‡], Thue W. Schwartz[‡], Andy Blanchard[§], Robert Jepras[§], and Mette M. Rosenkilde[‡1]

From the [‡]Laboratory for Molecular Pharmacology, Department of Neuroscience and Pharmacology, Faculty of Health Sciences, University of Copenhagen, Blegdamsvej 3, DK-2200 Copenhagen N, Denmark, [§]GlaxoSmithKline, Gunnels Wood Road, Stevenage SG1 2NY, United Kingdom, the [¶]Department of International Health, Immunology, and Microbiology, Faculty of Health Sciences, University of Copenhagen, Blegdamsvej 3, DK-2200 Copenhagen N, Denmark, and [‖]GlaxoSmithKline, Research Triangle Park, North Carolina 27709

The Epstein-Barr virus-induced receptor 2 (EBI2) is a constitutively active seven-transmembrane receptor, which was recently shown to orchestrate the positioning of B cells in the follicle. To date, no ligands, endogenously or synthetic, have been identified that modulate EBI2 activity. Here we describe an inverse agonist, GSK682753A, which selectively inhibited the constitutive activity of EBI2 with high potency and efficacy. In cAMP-response element-binding protein-based reporter and guanosine 5′-3-*O*-(thio)-triphosphate (GTPγS) binding assays, the potency of this compound was 2.6–53.6 nM, and its inhibitory efficacy was 75%. In addition, we show that EBI2 constitutively activated extracellular signal-regulated kinase (ERK) in a pertussis toxin-insensitive manner. Intriguingly, GSK682753A inhibited ERK phosphorylation, GTPγS binding, and cAMP-response element-binding protein activation with similar potency. Overexpression of EBI2 profoundly potentiated antibody-stimulated *ex vivo* proliferation of murine B cells compared with WT cells, whereas this was equivalently reduced for EBI2-deficient B cells. Inhibition of EBI2 constitutive activity suppressed the proliferation in all cases. Importantly, the suppression was of much higher potency (32-fold) in WT or EBI2-overexpressing B cells compared with EBI2-deficient counterparts. Finally, we screened GSK682753A against an EBI2 mutant library to determine putative molecular binding determinants in EBI2. We identified Phe^{111} at position III:08/3.32 as being crucial for GSK682753A inverse agonism because Ala substitution resulted in a >500-fold decrease in IC_{50}. In conclusion, we present the first ligand targeting EBI2. In turn, this molecule provides a useful tool for further characterization of EBI2 as well as serving as a potent lead compound.

The Epstein-Barr virus (EBV) induced receptor 2 (EBI2; also known as GPR183) is an orphan member of the 7TM[2] receptor family A. EBI2 is up-regulated up to 200-fold in B cells following EBV infection (1). In agreement with an expression pattern primarily restricted to immunological cell types (1, 2), it was recently demonstrated that EBI2 orchestrates the positioning of B cells in the follicle (3, 4). Specifically, expression of EBI2 allowed activated B cells to translocate to the outer follicular regions; in contrast, the absence of EBI2 permitted the cells to enter the germinal centers. Thus, EBI2 mediates the correct localization of B cells during humoral immune responses.

To date, no endogenous ligand for EBI2 has been identified. Given that this receptor does not have a close homolog, the chemical nature of such a ligand is difficult to infer. Accordingly, EBI2 has been placed in varying 7TM receptor subgroups by different phylogenetic analyses as being a target of peptide (1, 5) or lipid ligands (6). Nevertheless, many aspects of EBI2 signaling have been revealed. Thus, we have previously demonstrated that EBI2 is constitutively active through $G\alpha_i$ (but not $G\alpha_q$ or $G\alpha_s$) and serum response element (but not NFAT or NFκB) (2). In a subsequent mutational analysis, several functionally important residues were identified in various regions of the receptor; in particular, an Arg near the top of transmembrane II (TM-II) at position II:20/2.60 proved to be essential for EBI2 activity (7).

Constitutive activity as an *in vitro* phenomenon was first demonstrated by Costa and Herz (8) and has since been shown to be a physiologically relevant aspect of 7TM receptor signaling. For example, several naturally occurring activating mutations found in endogenous 7TM receptors have been linked to changes in phenotype or induction of pathogenesis. In addition to the many endogenous constitutively active 7TM receptors, several virus-encoded 7TM receptors are highly constitutively active, including the human cytomegalovirus (CMV)-encoded receptor US28 (9, 10), the human herpesvirus 8 (HHV8)-encoded ORF74 (11, 12), and the EBV-encoded BILF1 (13, 14). Although the precise role of the constitutive activity has to be fully elucidated, it has been speculated that it manipulates signaling pathways of the host cell in order to circumvent immune surveillance, thus increasing overall virus survival (15). Furthermore, in immune-compromised hosts, reactivation of a latent

[S] The on-line version of this article (available at http://www.jbc.org) contains supplemental Figs. 1–3.

[1] To whom correspondence should be addressed: Laboratory for Molecular Pharmacology, Dept. of Neuroscience and Pharmacology, Faculty of Health Sciences, University of Copenhagen, Blegdamsvej 3, DK-2200 Copenhagen N, Denmark. Tel.: 45-30604608; Fax: 45-35327610; E-mail: rosenkilde@sund.ku.dk.

[2] The abbreviations used are: 7TM, seven-transmembrane; CREB, cAMP-response element-binding protein; HHV8, human herpesvirus 8; PTLD, post-transplant lymphoproliferative disease; TM, transmembrane; GTPγS, guanosine 5′-3-*O*-(thio)triphosphate; BisTris, 2-[bis(2-hydroxyethyl)-amino]-2-(hydroxymethyl)propane-1,3-diol.

infection of these viruses can lead to severe disease even with fatal outcome like in CMV-encephalitis, HHV8-mediated Kaposi's sarcomas, and EBV-mediated lymphoproliferative disorders (15, 16). In the case of Kaposi's sarcoma, ORF74 is believed to be one of the primary oncogenes because transgenic mice expressing this receptor develop lesions closely resembling those of the human disease (17, 18) in agreement with its proliferative capability *in vitro* (11). Importantly, the constitutive activity of ORF74 was shown to be essential for this process because mice expressing non-constitutively active ORF74 mutants had a marked lower index of tumorigenesis (19). In support of this observation, cells expressing non-constitutively active US28 mutants were less efficient in promoting tumor development compared with WT counterparts when injected into nude mice (20). In turn, this indicates that US28 could function as an oncogene in CMV-related proliferative diseases. Finally, a recent study of BILF1 showed that also this receptor processes proliferative and cell transforming properties directly linked to its constitutive signaling (21).

Like HHV8 and CMV, EBV is associated with proliferative diseases, including infectious mononucleosis, nasopharyngeal carcinoma, Burkitt's lymphoma, and posttransplant lymphoproliferative disease (PTLD) (15, 22). The molecular key players in these diseases still have to be elucidated. However, given the association between 7TM receptor constitutive activity and tumorigenesis, combined with the marked increase in EBI2 expression levels upon EBV infection, we speculate that EBI2 might be one such player. In agreement with this, expression of EBI2 has been found to be elevated in EBV-positive compared with EBV-negative PTLD samples (23).

In this study, we present GSK682753A, the first ligand to target EBI2. GSK682753 served as a selective and highly potent inverse agonist for murine as well as human EBI2 with inhibition of G protein-dependent signals as well as signals that are probably G protein-independent. In addition, GSK682753A and two structurally related compounds (GSK682756A and SB477865) inhibited antibody-induced proliferation of murine WT B cells *ex vivo* more potently than EBI2-deficient counterparts. Finally, by mutational analysis and docking simulation, we propose a binding mode for GSK682753.

EXPERIMENTAL PROCEDURES

Materials

Murine EBI2 was cloned in-house using genomic DNA from murine spleen and corresponded to GenBank™ accession number NM_183031. Human EBI2 was kindly provided by H. R. Luttichau (University of Copenhagen) and corresponded to GenBank™ accession number NM_004951. The promiscuous chimeric G protein Gα6qi4myr (Gqi4myr) was kindly provided by Evi Kostenis (Rheinische Friedrich-Wilhelm University, Bonn, Germany). Lipofectamine™ 2000 reagent and Opti-MEM were purchased from Invitrogen. SteadyLite (Lyophilized Substrate Solution) was from Packard (Boston, MA). Goat anti-mouse horseradish peroxidase-conjugated antibody was from Pierce, whereas mouse anti-FLAG (M1) antibody, forskolin, and pertussis toxin were from Sigma. Both SlowFade antifade reagent and goat anti-mouse Alexa Fluor 488- and 568-conjugated antibodies were from Molecular Probes (Carlsbad, CA). The 3,3′,5,5′-tetramethylbenzidine substrate was purchased from KemEnTech (Taastrup, Denmark). GSK682753A was synthesized in-house at GlaxoSmithKline (Stevenage, United Kingdom) and dissolved in 100% DMSO.

Site-directed Mutagenesis

All EBI2 constructs were inserted into a modified pcDNA3 vector, kindly provided by Kate Hansen (7TM-Pharma, Lyngby, Denmark), which contained an upstream sequence encoding a hemagglutinin signal peptide fused to the FLAG tag. Site-directed mutagenesis was carried out using the *Pfu* polymerase (Stratagene), and the generated mutations were verified by bidirectional DNA sequencing at MWG Biotech (Martinsried, Germany).

Transfection and Tissue Culture

HEK293 cells were grown in DMEM adjusted to contain 4500 mg/liter glucose (Invitrogen, catalog no. 31966-021), 10% FBS (fetal bovine serum), 180 units/ml penicillin, and 45 μg/ml streptomycin (PenStrep) at 10% CO_2 and 37 °C. HEK293 cells stably transfected with M1-EBI2 WT were grown in the same medium but with G418 added at 800 mg/ml. For transient transfections, Lipofectamine™ 2000 reagent was used in the serum-free medium Opti-MEM according to the manufacturer's description. Briefly, the cells were transfected for 5 h at 37 °C using Lipofectamine™ 2000 at 12 μl/ml and receptor DNA or pcDNA3 at 15 ng/well and subsequently incubated in fresh growth medium containing GSK682753A at varying concentrations. HEK293 clones stably expressing FLAG-tagged WT EBI2 were generated by transfecting HEK293 cells with FLAG-tagged WT EBI2 cloned into pcDNA3 and selected using G418 (2).

CREB-based Reporting Luciferase Assay

The level of constitutive activity was determined using a CREB-based luciferase reporter assay according to the manufacturer's recommendations (Stratagene, La Jolla, CA). Cells were seeded at 35,000 cells/well in 96-well culture plates 24 h prior to transfection and were transfected with the trans-activator plasmid pFA2-CREB and the reporter plasmid pFRLUC at 6 and 50 ng/well, respectively, along with receptor DNA at 15 ng/well. In most experiments, the cells were co-transfected with the chimeric G protein, GαΔ6qi4myr (Gqi4myr) at 30 ng/well (24). However, as a more direct measurement of cAMP inhibition, forskolin (15 μM) was added instead of Gqi4myr, and the effect of GSK682753A on cAMP-induced CREB activation was measured. GSK682753A at varying concentrations was added when the transfection was stopped with a DMSO concentration after compound addition of 0.1%. The CREB activity was determined 24 h after transfection using the LucLite substrate (PerkinElmer Life Sciences). Briefly, the cells were washed twice in Dulbecco's PBS (0.9 mM $CaCl_2$, 2.7 mM KCl, 1.5 mM KH_2PO_4, 0.5 mM $MgCl_2$, 137 mM NaCl, and 8.1 mM Na_2HPO_4), and the luminescence was measured in a microplate scintillation and luminescence counter (Top-counter,

Packard) after a 10-min incubation in 100 μl of Dulbecco's PBS and 100 μl of Luc-Lite substrate.

Membrane Preparation

Membranes were prepared from naive HEK293 cells and HEK293 cells stably expressing FLAG-tagged EBI2 WT. The cells were manually harvested with a rubber policeman in ice-cold PBS and homogenized using a Dounce homogenizer on ice. The homogenate was centrifuged at 500 rpm for 3 min at 4 °C. Subsequently, the supernatants were collected and centrifuged at 20,000 rpm at 4 °C. The resulting membrane pellets were resuspended in 20 mM HEPES buffer containing 2 mM $MgCl_2$ and Complete protease inhibitor mixture (Roche Applied Science) and kept at −80 °C until subjected to [^{35}S]GTPγS binding experiments. The protein concentrations in each preparation were determined using the BCA protein assay kit (Pierce).

[^{35}S]GTPγS Binding Assay

[^{35}S]GTPγS binding experiments were carried out in white 96-well plates (Nunc) using the scintillation proximity assay-based method. A volume of membrane preparation (corresponding to 20 μg of protein/well) was diluted in assay buffer (final concentrations: 50 mM HEPES, 2 mM $MgCl_2$, 50 mM NaCl, 1 mM EGTA, 1 μM GDP, 0.1% BSA and Complete inhibitor mix). [^{35}S]GTPγS (PerkinElmer Life Sciences; 1250 Ci/mmol, 12.5 mCi/ml) diluted in assay buffer was added to a final concentration of 1 nM along with GSK682753A at varying concentrations and incubated for 30 min at room temperature. Subsequently, wheat germ agglutinin-coupled scintillation proximity assay beads (Amersham Biosciences) were added (final concentration of 2.8 mg/ml), followed by a 30-min incubation at room temperature on a plate shaker. Finally, the plates were centrifuged at 1500 rpm for 5 min, and the amount of radioactivity was determined using a Top Count scintillation counter (Packard Instruments). The level of nonspecific binding was determined by adding unlabeled GTPγS at a final concentration of 40 μM.

Enzyme-linked Immunosorbent Assay (ELISA)

HEK293 cells were transiently transfected with FLAG-tagged EBI2 WT at 15 ng/well using Lipofectamine™ 2000 as described above with GSK682753A at varying concentrations being added when the transfection was stopped. 24 h after transfection, the cells were fixed in 4% formaldehyde for 10 min, washed three times in TBS, and blocked for 30 min with TBS containing 2% BSA. Subsequently, the cells were incubated with mouse anti-FLAG M1 antibody at 2 μg/ml for 2 h in TBS supplemented with 1% BSA and 1 mM $CaCl_2$. After three washes in TBS containing 1% BSA and 1 mM $CaCl_2$, the cells were incubated for 1 h with goat anti-mouse horseradish peroxidase-conjugated antibody diluted 1:1000 in the same buffer as the primary antibody. Following washing, the immune reactivity was determined by the addition of 3,3′,5,5′-tetramethylbenzidine according to the manufacturer's instructions. All steps were carried out at room temperature.

Antibody-feeding Internalization Assay

HEK293 cells were seeded on poly-L-lysine-coated coverslips in 6-well plates at 5×10^5 cells/well. The following day, the cells were transfected with FLAG-tagged EBI2 WT at 150 ng/well using Lipofectamine™ 2000 as described above. 48 h after transfection, the cells were incubated in cold DMEM medium containing mouse M1 anti-FLAG antibody at 2 μg/ml and incubated for 1 h at 4 °C. After washing in cold DMEM medium, the specimens were either immediately fixed in 4% paraformaldehyde or incubated in prewarmed DMEM medium containing either vehicle (DMSO) or GSK682753A at 10 μM at 37 °C for 30 min to induce internalization and then fixed. Subsequently, the coverslips were blocked with TBS containing 2% BSA. To specifically detect labeled receptors still residing at the cell surface, the cells were incubated with goat anti-mouse Alexa Flour 488-conjugated antibody diluted 1:1000 in TBS containing 1% BSA for 30 min. After washing, the cells were permeabilized using TBS containing 1% BSA and 0.2% saponin for 30 min. To detect internalized labeled receptors, the coverslips were incubated with goat anti-mouse Alexa-Fluor 568-conjugated antibodies diluted 1:1000 in TBS containing 1% BSA for 30 min. Subsequent to washing, the specimens were mounted in SlowFade antifade reagent using nail polish as sealant. All steps following the internalization step were carried out at room temperature. Mock transfected cells were included to ensure no nonspecific binding of any of the antibodies.

Confocal Microscopy

Confocal microscopy was performed using an LSM 510 laser scanning unit coupled to an inverted microscope with a 63 × 1.4 numerical aperture oil immersion Plan-Apochromat objective (Carl Zeiss). Alexa-Fluor 488 was excited using an argon-krypton laser (λ = 488 nm), and the emission was collected with a 505-nm long pass filter. Images were recorded in 1024 × 1024 pixels and averaged over 16 whole frame scans.

Proliferation Assays

Using EBI2-overexpressing Mice—Mouse spleens were isolated from WT C57BL6J mice or transgenic mice overexpressing human EBI2 and kept in Hanks' medium on ice. Subsequently, pooled single cell suspensions were made, and B cells were isolated using mouse pan-T Dynabeads (Invitrogen). The purity and viability of the isolated B cells were evaluated using FACS and trypan blue, respectively, and were normally >90% in both cases. The cells were centrifuged and diluted in growth medium (RPMI 1640 containing 10% FBS and PenStrep) to 2×10^6 cells/ml. Following, 2×10^5 cells (100 μl) were added per well in 96-well flat bottom plates (COSTAR). 50 μl of medium containing inverse agonist at varying concentrations was then added (final DMSO concentration of 0.001%). For the anti-IgM dose-response experiments, 50 μl of medium was added instead. Finally, 50 μl of medium containing goat F(ab′)$_2$ polyclonal anti-mouse IgM (Abcam) was added. For inhibition experiments, the final anti-IgM concentration was 5.0 μg/ml, whereas this ranged from 0 to 10 μg/ml for the anti-IgM dose-response experiments. The cells were incubated 48 h before adding 1 μCi of [*methyl*-^{3}H]thymidine per well and incubated for an additional 16 h. The cells were finally harvested onto

96-well GF/C-filter plates (PerkinElmer), and 20 μl of MicroScint liquid scintillant was added to determine the amount of radioactivity using a TopCounter (Packard). Three mice were used per group in each experiment.

Using EBI2-deficient Mice—Mouse spleens were isolated from WT or EBI2-deficient C57BL6J mice and transferred into 6-well plates in 5 ml of culture medium (DMEM containing 10% FCS, 2 mM glutamine, penicillin, and streptomycin). Subsequently, single cell suspensions were made, followed by centrifugation at 1500 rpm for 5 min. Erythrocytes were lysed by resuspending the cell pellet in 2 ml/spleen M-Lyse buffer (R&D Systems) for 5 min. The reaction was stopped by adding 20 ml of culture medium. B cells were isolated from this suspension using a mouse B cell isolation kit. (R&D Systems) following the manufacturer's protocol. The purity of the isolated B cells was assessed by FACS using rat anti-mouse CD19-FITC (BD Biosciences) and was normally 80–90%. The isolated B cells were frozen down, stored in liquid nitrogen, and thawed on the day of the assay. Prior to assay, the viability of the cells was checked using trypan blue, normally being >90%. Thawed B cells were resuspended in culture medium to a concentration of 5×10^6 cells/ml. 50 μl of cell suspension (2.5×10^5 cells) was added per well in a 96-well flat bottom plate (COSTAR). Subsequently, prediluted and titrated compounds were added at 100 μl/well, giving a final DMSO concentration of 0.33%. The cells were incubated for 1 h at 37 °C before adding goat $F(ab')_2$ anti-mouse IgM (BIOSOURCE) in 50 μl of medium to a final concentration of 10 μg/ml. The plates were incubated for 48 h before adding [^{3}H]thymidine and were left for an additional 16 h. The cells were harvested onto glass fiber mats using a SKATRON 96-well harvester, dried, and sealed into polythene bags with liquid scintillant. The amount of incorporated radioactivity was determined using a microbeta counter (Wallac).

Chemotaxis

B cells from WT and EBI2-overexpressing mice were isolated as described for proliferation assays. The cells were resuspended at 10^7 cells/ml in chemotaxis buffer (RPMI 1640 + 0.5% BSA) containing either nothing, DMSO, or GSK682753A at 10 μM (final DMSO concentration of 0.01%). 10^6 cells (100 μl) were subsequently added to the upper chamber of a Transwell 12-well plate (Corning Glass), and 600 μl of the corresponding buffer was added to the lower chamber. The cells were incubated for 4 h at 37 °C, and the cells in the lower chamber were subsequently fixed in 4% paraformaldehyde. The number of cells migrated through the membrane was determined with FACS by gating on the lymphocyte population and counting the number of events within a 90-s time frame.

ERK Phosphorylation Assay

HEK293 cells were seeded out in 12-well plates at 350,000 cells/well and transiently transfected using the calcium phosphate method with FLAG-tagged EBI2 WT, β_2-adrenergic receptor, or pcDNA at 1.1 μg/well. When used, pertussis toxin (at 100 ng/ml) was administrated upon serum starvation. The cells were serum-starved overnight and incubated with GSK682753A at varying concentrations (for EBI2 and pcDNA) or isoproterenol at 1 μM (β_2-adrenergic receptor) for 10 min. Subsequently, the cells were washed twice in ice-cold PBS and lysed using lysis buffer (100 mM Tris, 4% SDS, 20% glycerol). The lysates were syringed and spun down for 5 min at 1500 rpm and 4 °C. The protein concentration was determined using a BCA protein kit (Pierce). A volume corresponding to 15–20 μg of protein was mixed with Western blot loading buffer and incubated for 2 min at 96 °C. Subsequently, the samples were loaded on BisTris 10% NuPAGE gels and run for 1.5 h at 140 V followed by blotting onto an ethanol-activated PVDF membrane for 1.5 h at 30 V. The membrane was then blocked in TBST (1× TBS with 0.1% Tween 20) containing 5% BSA for 1 h followed by a 1-h incubation in blocking buffer containing rabbit anti-phospho-ERK IgG antibody diluted 1:1000. After washing three times for 10 min with TBST, the membrane was incubated in blocking buffer containing goat anti-rabbit-IgG HRP-conjugated antibody diluted 1:10000 for 1 h. The membrane was washed and developed by incubating in SuperSignal West Pico substrate (Pierce) for 5 min. The amount of phosphorylation was measured using a FlourChem H2A camera. The membrane was subsequently stripped by incubating for 15 min in Pierce stripping buffer (Pierce) and washed three times in TBST. The procedure was then repeated with rabbit anti-ERK IgG antibody to detect total ERK. Image analysis and quantification were performed using AlphaEaseFC software.

RT-PCR

Total RNA was isolated from purified WT or EBI2-overexpressing B cells using the NucleoSpin RNA II kit (Macherey-Nagel). cDNA was synthesized from 0.5 μg of DNase-treated RNA using the ImProm II reverse transcriptase kit (Promega) and random hexamers (Roche Applied Science). A non-RT sample was included to examine possible genomic DNA contamination, of which none was detected. Qualitative transcript levels of hEBI2 and β-actin (copy normalizer) were assessed by amplifying 5 μl of cDNA by standard PCR (30 cycles). The products were run on an ethidium bromide-containing 2% agarose gel and visualized using UV light. Primers were as follows: hEBI2 forward, GCTTTGCCTACACGAATAGCCTACTATGCA; hEBI2 reverse, TCACTTTCCATTTGAAGACTTGG; β-actin forward, CGTCTTCCCCTCCATCGT; β-actin reverse, CGCCCACATAGGAATCCTTC. The experiment was performed twice.

Melanophore Assay

Melanophores were transiently transfected with cDNA encoding hEBI2 by electroporation and incubated overnight. The following day, cells were seeded into flat bottom half-well 96-well plates (COSTAR) at 14,000 cells/well and left for 2 h. After aspiration and the addition of melanophore assay buffer (L-15 Leibovitz medium containing 200 mM L-glutamine and 1% BSA), an initial transmittance read was taken using a SpectraMax plate reader. Compounds half-log serially diluted in assay buffer were then added (final DMSO concentration of 1%), the cells were incubated for 2 h, and a final read was taken. As controls, 100 nM α-Melanocyte Stimulating Hormone and/or 10 nM melanotonin were added. The results were normalized to the transmittance in the presence of melanotonin

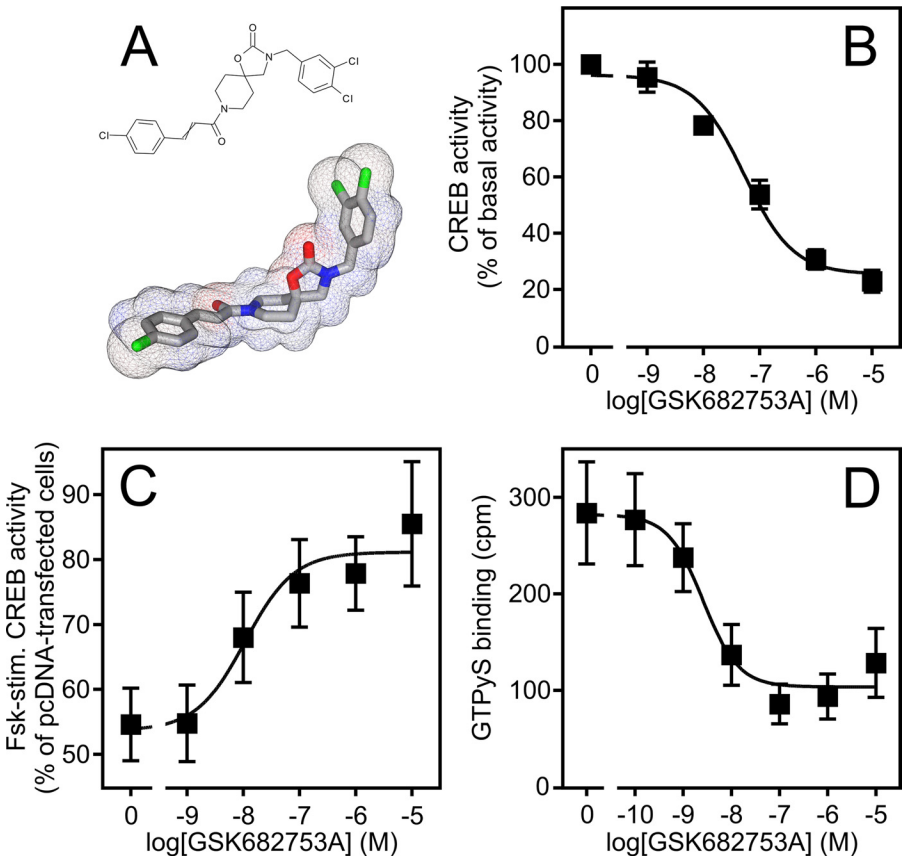

FIGURE 1. **Structure of the EBI2-selective inverse agonist GSK682753A.** *A*, two- and three-dimensional projections of GSK682753A generated using MarvinSketch and MarvinSpace software. *Red atoms*, oxygen; *blue atoms*, nitrogen; *green atoms*, chlorine. *B*, inhibition of EBI2 constitutive CREB activity by GSK682753A in HEK293 cells transiently transfected with FLAG-tagged EBI2 at 15 ng/well and the chimeric Gα subunit Gqi4myr at 30 ng/well. The results are subtracted for background (pcDNA-tranfected cells) and are presented as mean ± S.E. (*error bars*) in percent relative to the basal CREB activity at [GSK682753A] = 0 (DMSO only). The experiments were performed four independent times in quadruplicates. *C*, inhibition of forskolin-stimulated CREB activity by GSK682753A in HEK293 cells transiently transfected with FLAG-tagged EBI2 at 15 ng/well. Production of cAMP was stimulated with 15 mM forskolin. The results are presented as mean ± S.E. in percent relative to the CREB activity in forskolin-stimulated pcDNA-transfected cells and are from five independent experiments performed in quadruplicates. *D*, inhibition of [^{35}S]GTPγS binding to membranes isolated from FLAG-tagged EBI2-transfected HEK293 cells by GSK682753A. The results are subtracted for background (membranes from pcDNA-transfected cells) and are raw data presented as mean ± S.E. The experiments were performed six independent times in triplicates.

(100%) or α-Melanocyte Stimulating Hormone (0%). The experiments were performed at least twice in duplicates.

Data Handling

All results are presented as mean ± S.E. and are subtracted for background (pcDNA3-transfected cells). Potencies were determined using non-linear regression analysis in GraphPad Prism. All statistical analyses were performed using this program.

RESULTS

GSK682753A Inhibits the G Protein-dependent Constitutive Activity of EBI2 with High Potency without Affecting Cell Surface Expression—To identify an EBI2-specific inverse agonist, a library of piperidine-based, non-peptide molecules was screened, and the compound GSK682753A (IUPAC name 8-[(2E)-3-(4-chlorophenyl)prop-2-enoyl]-3-[(3,4-dichlorophenyl)methyl]-1-oxa-3,8-diazaspiro[4.5]decan-2-one) was found to be a hit (Fig. 1*A*). To characterize GSK682753A, we initially performed dose-response experiments using a CREB-based reporter assay in HEK293 cells transiently transfected with EBI2 WT and Gqi4myr, a chimeric Gα subunit that recognizes $G\alpha_i$-coupled receptors but activates $G\alpha_q$-regulated downstream pathways (24). GSK682753A dose-dependently inhibited the constitutive activity of EBI2 by up to 75% with an IC_{50} of 53.6 nM (pIC_{50} = 7.27 ± 0.12) (Fig. 1*B* and Table 1). Furthermore, a similar potency was observed for the murine EBI2 (supplemental Fig. 1). To determine specificity, GSK682753A was tested on several other constitutively active receptors, including GPR39, the ghrelin receptor, GPR17, MC1R, and ORF74; however, none of these were inhibited by GSK682753A concentrations up to 10 μM (data not shown). Because GPR17, which is the closest human homolog to EBI2, also signals constitutively through

TABLE 1

IC_{50} values for GSK682753A, GSK682756A, and SB477865 in three different assays

The essays were for CREB activity in the presence of Gqi4myr in HEK293 cells transfected with human EBI2 (IC_{50} in nM), transmittance of melanophores transfected with human EBI2 (IC_{50} in nM), and inhibition of antibody-induced proliferation of WT mouse B cells (IC_{50} in μM).

Compound	CREB assay	Melanophore	Proliferation
	nM	nM	μM
GSK682753A	53.6 ± 1.3	12.1 ± 1.4	1.3 ± 0.8
GSK682756A	57.0 ± 1.8	15.6 ± 1.1	0.3 ± 0.8
SB477865	71.5 ± 1.4	17.8 ± 1.2	1.6 ± 1.4

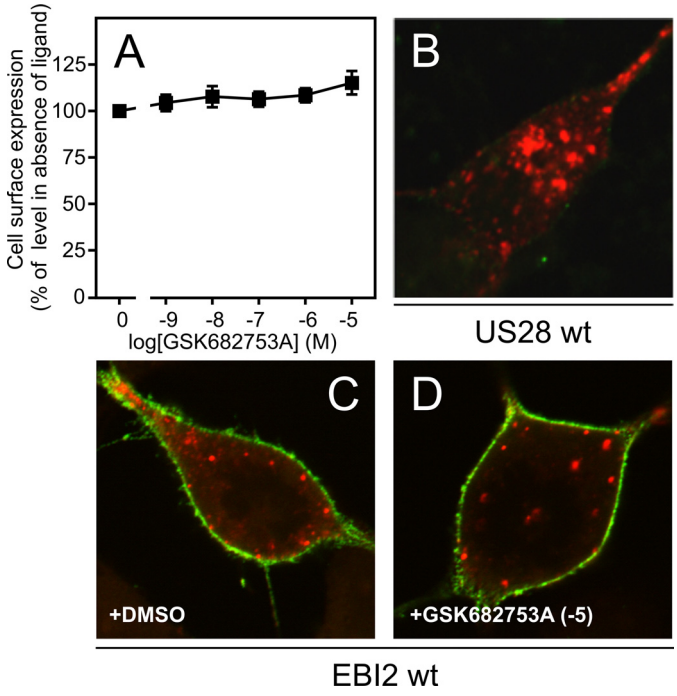

FIGURE 2. **GSK682753A does not affect cell surface expression (*A*) or constitutive internalization of EBI2 (*B–D*).** *A*, effect of GSK682753A on cell surface expression of FLAG-tagged EBI2 in HEK293 cells. The cells were transiently transfected with EBI2 at 15 ng/well, and the expression was measured using ELISA. The results are subtracted for background (pcDNA-transfected cells) and are presented as mean ± S.E. (*error bars*) in percent relative to the expression level at [GSK682753A] = 0 (DMSO only). The experiments were performed five independent times in quadruplicates. *B*, constitutive internalization of FLAG-tagged US28 in the presence of DMSO. *C* and *D*, constitutive internalization of FLAG-tagged EBI2 in the presence of DMSO (*C*) or 10 μM GSK682753A (*D*). Receptors at the surface were labeled with M1 anti-FLAG antibody prior to internalization. Subsequent to this, labeled receptors still residing at the cell surface were detected before permeabilization (*green*), and internalized receptors were detected after permeabilization (*red*) with two different secondary antibodies and analyzed by confocal microscopy. Mock transfected cells were used as control for nonspecific binding of both the primary and secondary antibodies, of which none was seen.

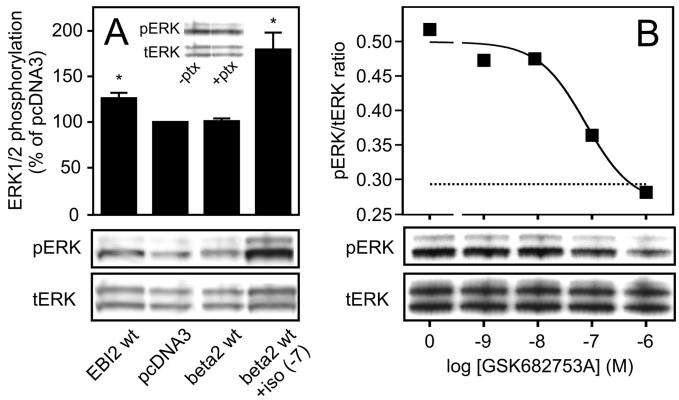

FIGURE 3. *A*, EBI2 is constitutively active via ERK. HEK293 cells were transiently transfected with EBI2 WT, β_2-adrenergic receptor (*beta2 wt*) or pcDNA3. The cells were serum-starved overnight before the start of the assay. Isoproterenol (*iso*) or vehicle was added to the β_2-adrenergic receptor at 100 nM for 10 min before cell lysing. The lysates were run on NuPAGE gels, blotted onto PVDF membranes, and probed for phospho-ERK or (after stripping) total ERK (*pERK* and *tERK*, respectively). The results are normalized to total ERK and are presented as a percentage relative to pcDNA3. A representative blot is shown at the *bottom*, and a *sum figure* of two independent experiments is shown at the *top*. *, $p < 0.05$ by Student's *t* test. *Inset*, pERK (*top*) and tERK (*bottom*) in the absence (*left*) or presence (*right*) of 100 ng/ml pertussis toxin (*ptx*). *B*, inhibition of ERK constitutive activity by GSK682753A. The amount of ERK phosphorylation was measured in transiently transfected HEK293 cells incubated for 10 min in the absence or presence of increasing concentrations of GSK682753A. A representative blot is shown at the *bottom*. The quantification of this is presented at the *top* as the ratio of phospho-ERK to total ERK. *Error bars*, S.E.

$G\alpha_i$ (25), this furthermore rules out the possibility of GSK682753A interfering directly with $G\alpha_i$ proteins. We subsequently performed the experiment in forskolin-stimulated HEK293 cells transfected with EBI2 in order to measure the potency of GSK682753A in the absence of Gqi4myr. Here, GSK682753A dose-dependently suppressed the inhibition of forskolin-stimulated cAMP accumulation mediated by EBI2 with an IC_{50} of 10.9 nM ($pIC_{50} = 7.96 \pm 0.50$) (Fig. 1*C*). Because transcription factor activation is a relatively far downstream event, the effect of GSK682753A was also measured at the level of G protein activation. We have previously shown that the constitutive activity of EBI2 can be measured by determining the level of [^{35}S]GTPγS binding to membranes isolated from cells stably expressing EBI2 (7). Thus, we determined the GTPγS binding in the presence of increasing concentrations of GSK682753A. As observed in the two previous experiments, GSK682753A inhibited the binding of GTPγS to EBI2-containing membranes in a dose-dependent fashion with an IC_{50} of 2.6 nM (Fig. 1*D*).

In order to ensure that the inhibition of EBI2 constitutive activity was not a matter of altered surface expression, the expression level of EBI2 was determined in the presence of the compound. However, GSK682753A did not affect the cell surface expression of EBI2 in HEK293 cells even at a concentration of 10 μM (Fig. 2*A*). To examine whether GSK682753A influenced the constitutive internalization of EBI2, we measured the internalization rate using an antibody-feeding assay. GSK682753A did not affect the internalization because the relative amount of internalized receptors (*red dots*) after the incubation period remained unaltered whether or not GSK682753A was present (Fig. 2, *C* and *D*). US28 was included as a control because it constitutively internalizes at a fast rate, and accordingly, virtually all receptors were internalized (Fig. 2*B*) (26). No internalization was observed when the cells were fixed prior to incubation (data not shown).

GSK682753A Inhibits EBI2-mediated Constitutive ERK Activity—In contrast to the previously described constitutive activation of $G\alpha_i$ (2), it has not been determined whether EBI2 also constitutively activates MAPKs. Therefore, we tested whether EBI2 constitutively activates the ERK1/2 kinases. As shown in Fig. 3*A*, EBI2 indeed activated ERK up to 30% over base line, which corresponded to 36% of the isoproterenol-mediated stimulation of the β_2-adrenergic receptor. Furthermore, this activity was not affected by the presence of the $G\alpha_i$ inhibitor pertussis toxin (*ptx*; Fig. 3*A*, *inset*) and thus probably reflects G protein-independent signaling, although putative ERK activation via G proteins other than $G\alpha_i$ cannot completely be ruled out. To determine whether GSK682753A inhibited this activity or alternatively stimulated this in a biased mode of action, we measured ERK phosphorylation levels in the presence of increasing GSK682753A concentrations. We found that GSK682753A inhibited EBI2-mediated ERK phosphorylation in a dose-dependent fashion with an IC_{50} of 76 nM, demonstrat-

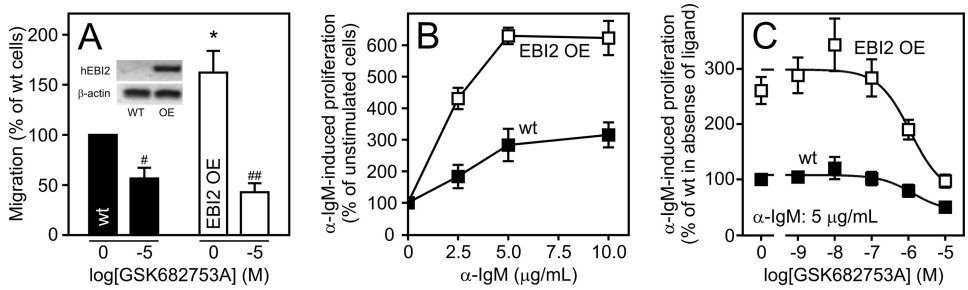

FIGURE 4. **Overexpression of EBI2 increases basal B cell migration and potentiates antibody-induced B cell proliferation.** *A*, B cells isolated from WT mice (*black bars*) or transgenic mice overexpressing human EBI2 (*EBI2 OE*, *white bars*) were seeded in Transwell chemotaxis plates and incubated for 4 h in the presence of DMSO (0) or GSK682753A (10 μM). The number of cells that migrated through the membrane was subsequently determined by FACS. The data are normalized to the migration of WT B cells in the absence of GSK682753A and are the sum of three independent experiments performed in duplicates. #, $p < 0.05$; ##, $p < 0.01$; vehicle *versus* ligand-treated cells. *, $p < 0.05$; vehicle-treated WT *versus* vehicle-treated EBI2-overexpressing cells. All are Student's *t* test. *Inset*, expression of hEBI2 (*top*) and β-actin (*bottom*) in WT (*left*) and EBI2-overexpressing B cells (*right*) as measured by RT-PCR. *B*, B cells isolated from WT or EBI2-overexpressing mice were stimulated with increasing amounts of goat F(ab')$_2$ anti-IgM to induce proliferation. The data are normalized to the level of proliferation of unstimulated cells in percent and are the sum of three independent experiments performed in duplicates. *C*, B cells isolated from WT mice or transgenic mice overexpressing human EBI2 were stimulated with 5 μg/ml goat F(ab')$_2$ anti-IgM in the presence of vehicle (DMSO, [GSK682753A] = 0) or increasing amounts of GSK682753A. The data are normalized to the proliferation of WT B cells in the absence of GSK682753A in percent and are the sum of four independent experiments performed in triplicates. *Error bars*, S.E.

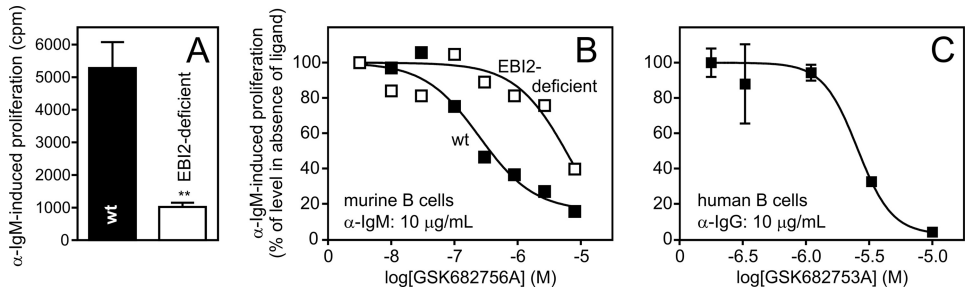

FIGURE 5. **Inhibition of antibody-induced proliferation of WT and EBI2-deficient B cells.** *A*, proliferation of WT and EBI2-deficient B cells. The results are raw results from one representative experiment of two. **, $p < 0.01$. *B*, B cells isolated from WT or EBI2-deficient mice were treated with goat F(ab')$_2$ anti-IgM (10 μg/ml) to induce proliferation in the absence or presence of increasing amounts of GSK682756A. The data are normalized to the level of proliferation in the absence of GSK682756A in percent. One representative experiment of two is shown. *C*, B cells isolated from healthy human donors were treated with anti-IgG (10 μg/ml) to induce proliferation in the absence or presence of increasing amounts of GSK682753A. The data are normalized to the level of proliferation in the absence of GSK682753A in percent. One representative experiment of two is shown. *Error bars*, S.E.

ing that GSK682753A functioned as an inverse agonist for both $G\alpha_i$ and the ERK1/2 pathway (Fig. 3*B*).

The Expression Level of EBI2 Modulates Antibody-induced B Cell Proliferation, Which Can Be Suppressed by EBI2 Inverse Agonism—We have previously generated a mouse overexpressing human EBI2 specifically in B cells (Fig. 4*A*, *inset*) to mimic the expression pattern observed upon EBV infection. We initially examined whether overexpression of EBI2 (and hence a higher level of constitutive activity) leads to increased basal migration of B cells *ex vivo*. As shown in Fig. 4*A*, EBI2 overexpression (*OE*) results in a significant increase (1.5-fold) in migration in line with this receptor controlling B cell migration in the follicle (3, 4). Furthermore, for both WT and overexpressing cells, the migration was inhibited by GSK682753A to ~50% of WT B cells. Next, to test if EBI2 overexpression putatively modulates B cell proliferation, we measured the rate of antibody-induced proliferation *ex vivo*. Thus, B cells isolated from WT or EBI2-overexpressing mice were stimulated with increasing amounts of an anti-IgM F(ab')$_2$ fragment. As seen in Fig. 4*B*, the antibody dose-dependently induced proliferation of both WT and EBI2-overexpressing B cells. However, the proliferation of the latter was profoundly increased compared with the former, being increased 3-fold. To test whether the proliferation could be suppressed EBI2 inverse agonism, we measured the proliferation in the presence of GSK682753A. For both WT and EBI2-overexpressing B cells, the proliferation was dose-dependently inhibited with IC_{50} values of 1.3 and 1.1 μM, respectively (Fig. 4*C*). Notably, GSK682753A suppressed the proliferation of EBI2-overexpressing B cells almost to the level of WT cells. To study the putative role of EBI2 in B cell proliferation further, we next measured the antibody-induced proliferation of EBI2-deficient B cells. Notably, in agreement with the increased proliferation of EBI2-overexpressing B cells, the proliferation of EBI2-deficient B cells was reduced 5-fold compared with WT counterparts (Fig. 5*A*). Furthermore, to validate the specificity of the inverse agonist-mediated inhibition of proliferation, we tested this in EBI2-deficient B cells. In these experiments, we used the compound GSK682756A, which is structurally highly similar to GSK682753A, binds in a similar mode, and inhibits the constitutive activity of EBI2 with equivalent potency and efficacy (Table 1 and supplemental Figs. 1 and 2). As seen in Fig. 5*A*, GSK682756A inhibited the B cell proliferation in a dose-dependent manner. Importantly, GSK682756A was markedly more potent on WT B cells compared with EBI2-deficient B cells, having IC_{50} values of 0.28 and 8.4 μM, respectively. Moreover, a similar result was obtained with SB477865, another structurally and pharmacologically equivalent EBI2 inverse agonist (Table 1 and supplemental Figs. 1 and 3). To determine whether this observation also extended to human EBI2, we measured the effect of GSK682753A on

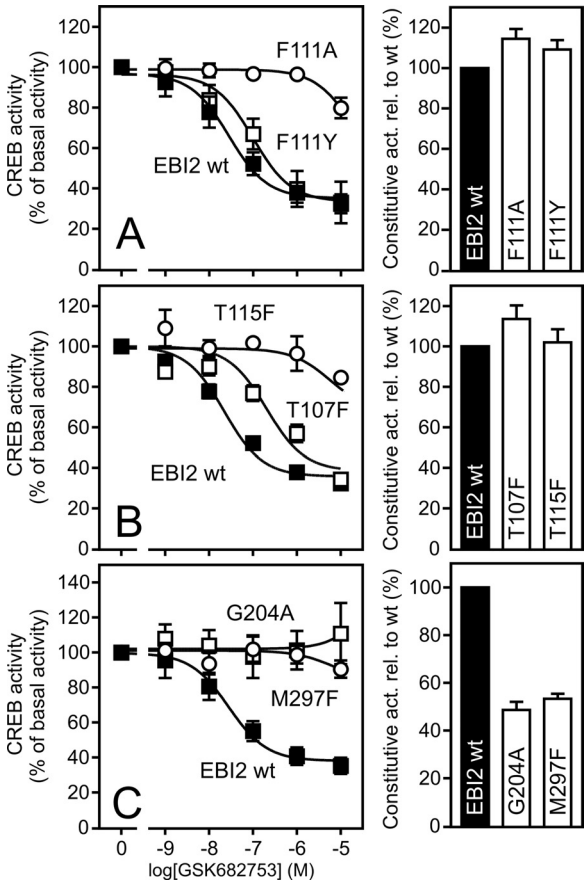

FIGURE 6. **Inhibition of constitutive CREB activity of EBI2 WT and selected mutants by GSK682753A.** *A*, effect of GSK682753A on Ala and Tyr substitutions of the TM-III residue Phe^{111} (F111A and F111Y, position III:08/3.32) in HEK293 cells transiently transfected with receptor construct at 15 ng/well and Gqi4myr at 30 ng/well (*left*). The background-subtracted results are presented as mean ± S.E. (*error bars*) in percent relative to the activity at [GSK682753A] = 0 and are from 3–4 independent experiments performed in quadruplicates. The constitutive activity of the mutants relative to that of EBI2 WT is presented to the *right*. *B*, effect of GSK682753A on Phe substitutions of the TM-III residues Thr^{107} (T107F, position III:04/3.28) and Thr^{115} (T115F, III:12/3.36), performed and presented as in *A*. *C*, effect of GSK682753A on Ala substitution of the TM-V residue Gly^{204} (G204A, position V:12/5.46) and Phe substitution of the TM-VII residue Met^{297} (M297F, VII:09/7.42), performed and presented as in *A*.

anti-IgG-induced proliferation of human B cells. In agreement with the observations in murine B cells, inhibiting human EBI2 constitutive activity resulted in a dose-dependent decrease in B cell proliferation with an IC_{50} of 3.0 μM (Fig. 5*B*).

Mutational Mapping of GSK682753A Binding to EBI2—The molecular interaction of GSK682753A was examined by screening a library of EBI2 mutations using the CREB-based assay. We initially focused on TM-III because it is known to be one of the key players in 7TM receptor activation, during which the top of this helix has been hypothesized to perform an inward see-saw movement, as described in the global toggle switch model (27–29). Specifically, position III:08/3.32 in TM-III has been shown to be important for ligand binding and helical movement as seen in, for example, the β-adrenergic subfamily (30). In EBI2, a Phe (Phe^{111}) is found this position. Ala substitution of this residue only slightly affects the constitutive activity of the receptor, thus not being important for the constitutive activity in general (Fig. 6*A*, *right*) (7). However, in contrast to the insignificant effect on constitutive activity, Ala substitution had a profound impact on GSK682753A inverse agonism. Thus, the suppression of constitutive activity mediated by the compound was essentially lost in this mutant, with a >500-fold decrease in potency (Fig. 6*A* and Table 2). On the contrary, virtually no effect on potency or efficacy was observed for the Tyr mutant, suggesting that an aromatic side chain at III:08/3.32 is required for GSK682753A action.

We next screened the residues located one helix turn above and below Phe^{111} at positions III:04/3.28 (Thr^{107}) and III:12/3.36 (Thr^{115}), respectively. These residues do not seem to be directly involved in GSK682753A action because the corresponding Ala mutants exhibited WT-like potency (Table 2). However, when mutated to a Phe, a profound decrease in potency was observed with an ~190-fold reduction for Thr^{115} (Fig. 6*B* and Table 2). For Thr^{107}, a more modest decrease was observed (10-fold). Furthermore, the same phenomenon was observed for Met^{297} at position VII:09/7.42 in TM-VII, a residue located close to III:08/3.32, where Ala substitution at VII:09/7.42 had no effect on the potency of GSK682753A, but introducing a Phe fully impaired the inhibition (Fig. 6*C* and Table 2). Thus, collectively, the results suggest that GSK682753A is located in close proximity to these residues.

Residue V:12 has previously been shown to be important for the action of small molecule ligands in, for example, CCR8 (31). As in CCR8, a Gly is found at this position in EBI2. Intriguingly, replacing the Gly with an Ala completely destroyed the ability of GSK682753A to suppress EBI2 constitutive activity (Fig. 6*C*). Given that Gly is an achiral amino acid, it is evident that Gly^{204} is not involved in an interaction with GSK682753A but rather plays a structural role. In addition, we tested several other residues of importance for 7TM receptor activation in TM-II, -V, -VI, and -VII; however, none of these significantly altered the potency of GSK682753A (Table 2).

To further explore the mode of GSK682753A binding to EBI2, we performed a docking simulation (32) using a homology model of EBI2 based on the crystal structure of bovine rhodopsin. As shown in Fig. 7*B*, the simulation suggested that when GSK682753A is bound to EBI2, it assumes a bent, "L-shaped" conformation similar to that observed in its lowest energy state (Fig. 1*A*). Thus, one part of the molecule is horizontally aligned, whereas the other part is aligned with and located close to TM-V. Of note, the mono-chloro-substituted phenyl ring of GSK682753A makes a slightly distorted edge-to-face interaction with the phenyl ring of Phe^{111} (Fig. 7). Specifically, the partial negative charge of the chlorine atom is positioned to interact with the partial positive charge of one or more hydrogen atoms of the Phe^{111} phenyl group (*red dotted lines*). This interaction corresponds well with the observation that Phe^{111} is essential for the action of GSK682753A (Fig. 6*A*). Also, the close proximity of GSK682753A with TM-V agrees with the observation that Gly^{204} (and perhaps the conformation of TM-V in general) is of functional importance to GSK682753A.

DISCUSSION

In this study, we identify and pharmacologically characterize GSK682753A, the first ligand known to target EBI2. This compound inhibited the $G\alpha_i$-dependent constitutive activity of

TABLE 2

Inhibition of constitutive activity of EBI2 WT and mutants by GSK682753A in HEK293 cells co-transfected with Gqi4myr

pIC_{50} ($-logIC_{50}$) is provided together with basal (constitutive) activity for each mutation and the maximum inhibition by GSK682753A given as a percentage of basal activity of EBI2 WT. These values are given as the mean ± S.E. The -fold change in potency (ΔIC_{50}) was compared with the WT EBI2 IC_{50}. *n* is the number of independent experiments performed. NA, not available.

	Residue	Position	Mutation	IC_{50} ($-logIC_{50}$)	Basal constitutive activity	Maximum inhibition	ΔIC_{50}	*n*
					%[a]	%[b]		
EBI2 WT				−7.3 ± 0.12	96.3 ± 2.77	25.5 ± 3.16	1.0	5
TM-II	Phe^{80}	II:13/2.53	F(II:13)A	−8.1 ± 0.35	101.1 ± 5.03	50.5 ± 5.72	0.1	4
	Leu^{84}	II:17/2.57	L(II:17)A	−8.2 ± 0.20	93.3 ± 3.63	29.8 ± 4.11	0.1	4
	Tyr^{91}	II:24/2.64	Y(II:24)A	−7.9 ± 0.24	109.8 ± 4.70	37.9 ± 5.83	0.3	4
TM-III	Thr^{107}	III:04/3.28	T(III:04)A	−7.6 ± 0.24	89.9 ± 5.07	8.8 ± 7.72	0.5	5
	T(III:04)F	−6.3 ± 0.24	104.3 ± 3.89	NA	8.6	3		
	Phe^{111}	III:08/3.32	F(III:08)A	−4.5 ± 0.32	113.1 ± 3.96	NA	564.9	4
			F(III:08)Y	−7.0 ± 0.20	106.0 ± 3.45	35.8 ± 5.95	1.7	3
	Thr^{115}	III:12/3.36	T(III:12)A	−9.7 ± 0.74	109.5 ± 9.72	73.7 ± 6.31	0.0	4
			T(III:12)F	−5.0 ± 2.35	108.4 ± 2.96	70.3 ± 1.05	186.2	3
TM-V	Cys^{201}	V:09/5.43	C(V:09)A	−8.3 ± 0.14	121.4 ± 3.18	41.3 ± 3.46	0.1	4
			C(V:09)S	−8.3 ± 0.13	121.8 ± 2.97	38.9 ± 3.23	0.1	4
	Gly^{204}	V:12/5.46	G(V:12)A	NA	48.5 ± 1.93	NA	NA	4
	Tyr^{205}	V:13/5.47	Y(V:13)A	−8.6 ± 0.16	69.2 ± 2.73	10.3 ± 2.60	0.0	4
			Y(V:13)F	−8.2 ± 0.28	109.9 ± 3.88	61.0 ± 4.30	0.1	4
TM-VI	Phe^{253}	VI:09/6.44	F(VI:09)A	−8.1 ± 0.31	76.8 ± 3.80	33.8 ± 4.38	0.1	5
	Phe^{257}	VI:13/6.48	F(VI:13)W	−8.5 ± 0.18	80.3 ± 2.97	22.9 ± 2.99	0.1	4
	Tyr^{260}	VI:16/6.51	Y(VI:16)A	−8.3 ± 0.69	17.9 ± 1.20	11.8 ± 1.28	0.1	4
			Y(VI:16)F	−8.8 ± 0.15	42.0 ± 1.39	13.2 ± 1.25	0.0	4
TM-VII	Val^{294}	VII:06/7.39	V(VII:06)A	−7.9 ± 0.20	105.0 ± 3.83	37.5 ± 4.65	0.2	4
	Met^{297}	VII:09/7.42	M(VII:09)A	−7.9 ± 0.14	86.2 ± 3.06	10.3 ± 3.69	0.2	4
			M(VII:09)F	NA	54.6 ± 6.46	NA	NA	4

[a] % of WT constitutive activity.
[b] % of basal constitutive activity for each mutation.

EBI2 with high potency and efficacy (Fig. 1). In addition, we found that EBI2 constitutively activated ERK in a pertussis toxin-insensitive manner and that GSK682753A also inhibited this activity (Fig. 3). Furthermore, overexpression of EBI2 potentiated antibody-induced *ex vivo* proliferation up to 3-fold, which was suppressed to WT level by GSK682753A (Fig. 4). Importantly, the inverse agonist-mediated inhibition of EBI2 suppressed the proliferation of WT B cells more potently than that of EBI2-deficient B cells (Fig. 5). It should be noted that the potencies of the ligands vary between the *in vitro* and *ex vivo* experiments (Table 1). This is probably due to the difference in cellular context including variation in, for example, the G protein expression level, which is known to affect ligand potency (33). Also, whereas the G protein activation is mediated directly by EBI2, the proliferation is induced by antibody-mediated B-cell receptor cross-linking and thus involves a multitude of signaling pathways.

We initially determined the ability of GSK682753A to suppress the $G\alpha_i$-dependent constitutive activity of EBI2 *in vitro*. Specifically, we measured the inhibition both close to (GTPγS assay; Fig. 1*D*) and far downstream (CREB reporter assays; Fig. 1, *B* and *C*) from the initial ligand binding event. This approach rules out the possibility that GSK682753A simply interferes nonspecifically with downstream signaling components and suggests that the inhibition indeed is a result of a receptor-ligand interaction. Importantly, GSK682753A did not affect the constitutive activity of a panel of virus-encoded and endogenous 7TM receptors (including GPR17, the closest human homolog to EBI2), suggesting that GSK682753A is selectively targeting EBI2. This is further emphasized by the observation that GSK682756A, a compound structurally and pharmacologically similar to GSK682753A (Table 1 and supplemental Fig. 1), was much more potent in inhibiting the antibody-induced proliferation of murine WT B cells compared with EBI2-deficient counterparts (Fig. 5*A*). It should be noted, however, that GSK682756A to some degree still inhibits the proliferation of EBI2-deficient B cells at high concentrations, indicating low potency off-target activity under these circumstances.

One concern regarding constitutive activity is that it could merely be a result of the presence of an agonist in the medium. Hence, an inverse agonist would in that case rather function as an antagonist. In the case of EBI2, however, the fact that constitutive activity has been observed in two different functional assays (CREB reporter and GTPγS assays) suggests that this is not an artifact.

It is well appreciated that many 7TM receptors signal not only via G proteins but also through other cellular effectors, including arrestins and, further downstream, the MAPK pathways. Importantly, these different signaling pathways regulate distinct physiological processes (34). This is exemplified well by GPR109A, which is activated by nicotinic acid and signals both through $G\alpha_i$ and β-arrestin. However, it is the G protein-dependent signaling that mediates the anti-lipolytic effect of nicotinic acid, whereas the flushing is mediated by the G protein-independent signaling in cutaneous Langerhans cells (35). Besides signaling though $G\alpha_i$, we found that EBI2 also signals constitutively via ERK (Fig. 3), and it will be interesting to see whether EBI2, like GPR109A, regulates distinct processes via these different effectors. Moreover, GSK682753A is able to suppress this activity with high potency and is thus an inverse agonist at both pathways, as seen in the α_{1D}-adrenergic receptor, where the inverse agonist prazosin suppresses the activity of the $G\alpha_q$ as well as the ERK pathways (36). On the other hand, the results are contradictory to the biased pharmacological profile of the β_2-adrenergic ligand ICI118551 that functions as an inverse agonist at the $G\alpha_s$ pathway and as an agonist at the ERK pathway (37).

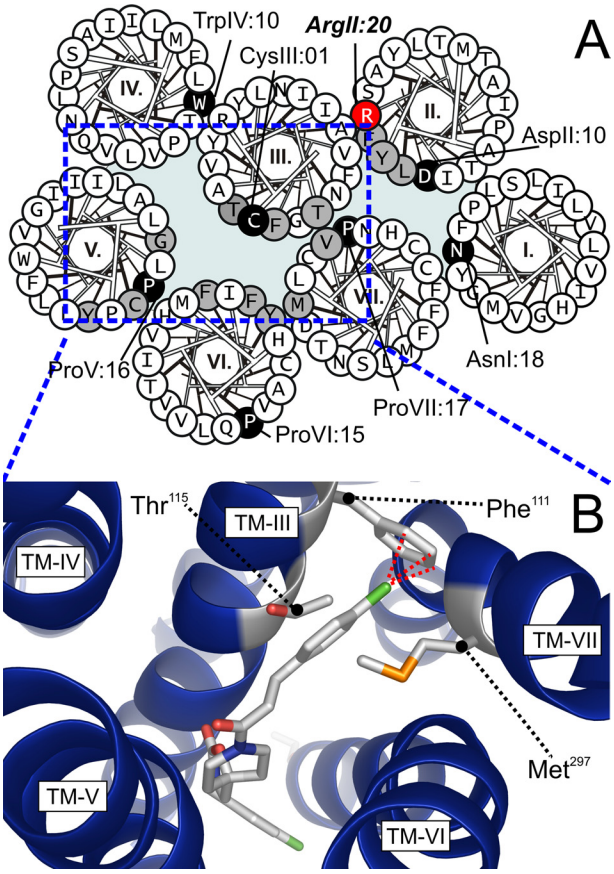

FIGURE 7. **Helical wheel and docking model of GSK682753A binding to EBI2.** *A*, helical wheel model of EBI2 with residues mutated in this study in *gray* and conserved residues in *black*. ArgII:20, with a recently identified role in EBI2 constitutive activity, is indicated in *red*. *B*, docking model generated with AutoDock Vina and an EBI2 model based on the crystal structure of bovine rhodopsin. Phe^{111} (III:08/3.32) and Met^{297} (VII:09/7.42) were set to be conformationally flexible. The search space covered the center of the main binding pocket. The viewpoint is extracellular with GSK682753A bound in the main binding pocket. The side chains of residues Phe^{111}, Thr^{115}, and Met^{297} are indicated. The *red dashed lines* show possible dipole interactions between the chlorine atom and one or more of the hydrogen atoms in the Phe^{111} phenyl ring.

The mapping and docking results indicated that GSK682753A interacts with residues facing the major binding pocket (Table 2 and Fig. 7). Phe^{111} appears to be directly involved in GSK682753A binding and not indirectly as, for example, part of conformational changes because Ala-substitution of this residue does not affect the constitutive activity *per se* (Fig. 6*A*) (7). This is supported by our docking model in which the mono-chloro-substituted phenyl group of GSK682753A forms an edge-to-face aromatic interaction with Phe^{111} (Fig. 7*B*). These results are in good agreement with the notion that position III:08/3.32 is crucial to many 7TM receptors. For example, the monoamine receptors contain an Asp at position III:08/3.32 that interacts with the quaternary amine of the monoamine ligand (30, 38–40). Also, III:08/3.32 constitutes a crucial part of activating bi- and tridentate metal ion binding sites engineered into the β_2-adrenergic receptor (27) and also serves as an anchor point for C5a binding to the C5a receptor (41) as well as for most chemokines and small molecule agonists targeting chemokine receptors (42). We also found that Phe-substitution of Thr^{115} at position III:12/3.36 and Met^{297} at VII:09/7.42 completely destroyed the GSK682753A-mediated inhibition, whereas Ala substitution did not (Fig. 6, *B* and *C*). Given that these residues are located one helix turn below Phe^{111}, one can speculate that a bulky side chain at III:12/3.36 or VII:09/7.42 may prevent GSK682753A from interacting with this residue by steric hindrance, as also suggested by the docking model (Fig. 7*B*). Upon 7TM receptor activation, the top of TM-III and -VI move closer, and it has been speculated that an inverse agonist functions as a wedge preventing these helices from approaching each other (28, 29). In agreement with this hypothesis, it has been shown that III:04/3.36 and VII:09/7.42 in fact move close together upon activation of the M3 muscarinic receptor (43). Thus, given that GSK682753A probably resides between these residues, it can be speculated that the compound inhibits the constitutive activity of EBI2 by preventing TM-III and -VII from approaching each other.

The physiological role of EBI2 constitutive activity remains to be elucidated. It is rather unlikely that it plays a role in the B cell migration in the follicle, which requires a chemical gradient. This is more likely mediated by a hitherto unidentified endogenous agonist. Supporting this, unpublished observations from Pereira *et al.* (44) suggest that an agonist indeed exists and probably is of a lipid-like nature. However, EBI2 might exert a range of pleiotropic effects, some of which could be regulated by its constitutive activity. For instance, it may modulate the proliferation rate of B cells as observed in this study, where a higher expression level (and hence a higher level of constitutive activity) and EBI2 deficiency were shown to potentiate and reduce the proliferation rate, respectively (Figs. 4 and 5).

In addition to its physiological role, EBI2 may also be involved in pathological settings. Thus, EBV seropositivity is etiologically associated with a range of proliferative malignancies in both immunocompetent and immunocompromised individuals, including several lymphomas and carcinomas (15, 22). This agrees well with the observation that EBV infection of B cells *in vitro* leads to transformation of the infected cells into highly proliferative immortalized lymphoblastoid cell lines. In patients receiving immunosuppressive treatment, the immune system is weakened and incapable of raising an appropriate response in general. Thus, in such patients, reactivation of latent EBV can lead to the uncontrolled proliferation of EBV-infected B cells due to an insufficient T-cell response and ultimately lymphoma development. An example of this is seen in the case of PTLD. This condition encompasses a range of histologically related disorders and develops in 2–24% of transplantation patients, depending on the transplant type. Furthermore, more than 95% of the PTLDs that occur within the first year after transplantation are thought to be EBV-related, underscoring the crucial role of EBV in the early development of this condition (45). It has been proposed that the development of PTLD *in vivo* probably resembles that of EBV-mediated transformation of B cells *in vitro* because the gene expression pattern of EBV genes in these conditions is similar. Specifically, under these circumstances EBV expresses the genes of the latency III program (22). It is interesting to note that the expression of EBI2 is massively up-regulated under this program, as seen both *in vitro* (1, 46) and in EBV-positive PTLD

samples (23). Given the association between 7TM receptor constitutive activity and tumorigenesis (11, 19), it is tempting to speculate that EBI2 in PTLD and other latency III-associated diseases could function as an oncogene. This is substantiated by the observation that overexpression of EBI2 profoundly potentiates the antibody-induced proliferation rate of B cells, whereas EBI2 deficiency has the opposite effect (Figs. 4 and 5). Furthermore, this proliferation was suppressed by inhibition of the EBI2 constitutive activity in both murine and human B cells and with specificity because the potency was much lower in EBI2-deficient cells (Figs. 4 and 5). Thus, collectively, these observations suggest that EBI2, besides being involved in the follicular localization, may also be important for the proliferation of activated B cells. In turn, EBI2, when expressed at high levels, might contribute to the transformation and uncontrolled expansion of EBV-infected B cells in immunocompromised individuals, ultimately leading to tumorigenesis as observed for ORF74.

In conclusion, GSK682753A serves as a promising lead compound for a potent EBI2-selective inverse agonist. In addition, it may be useful for further defining the role of EBI2 in physiological and pathological settings.

Acknowledgments—T. B.-J. and M. M. R thank Inger Smith Simonsen for excellent technical assistance and Ulrik Gether for use of the confocal microscope and the FlourChem H2A camera.

REFERENCES

1. Birkenbach, M., Josefsen, K., Yalamanchili, R., Lenoir, G., and Kieff, E. (1993) *J. Virol.* **67,** 2209–2220
2. Rosenkilde, M. M., Benned-Jensen, T., Andersen, H., Holst, P. J., Kledal, T. N., Lüttichau, H. R., Larsen, J. K., Christensen, J. P., and Schwartz, T. W. (2006) *J. Biol. Chem.* **281,** 13199–13208
3. Gatto, D., Paus, D., Basten, A., Mackay, C. R., and Brink, R. (2009) *Immunity* **31,** 259–269
4. Pereira, J. P., Kelly, L. M., Xu, Y., and Cyster, J. G. (2009) *Nature* **460,** 1122–1126
5. Lapinsh, M., Gutcaits, A., Prusis, P., Post, C., Lundstedt, T., and Wikberg, J. E. (2002) *Protein Sci.* **11,** 795–805
6. Joost, P., and Methner, A. (2002) *Genome Biol.* **3,** RESEARCH0063
7. Benned-Jensen, T., and Rosenkilde, M. M. (2008) *Mol. Pharmacol.* **74,** 1008–1021
8. Costa, T., and Herz, A. (1989) *Proc. Natl. Acad. Sci.* **86,** 7321–7325
9. Casarosa, P., Bakker, R. A., Verzijl, D., Navis, M., Timmerman, H., Leurs, R., and Smit, M. J. (2001) *J. Biol. Chem.* **276,** 1133–1137
10. Kledal, T. N., Rosenkilde, M. M., and Schwartz, T. W. (1998) *FEBS Lett.* **441,** 209–214
11. Arvanitakis, L., Geras-Raaka, E., Varma, A., Gershengorn, M. C., and Cesarman, E. (1997) *Nature* **385,** 347–350
12. Rosenkilde, M. M., Kledal, T. N., Bräuner-Osborne, H., and Schwartz, T. W. (1999) *J. Biol. Chem.* **274,** 956–961
13. Beisser, P. S., Verzijl, D., Gruijthuijsen, Y. K., Beuken, E., Smit, M. J., Leurs, R., Bruggeman, C. A., and Vink, C. (2005) *J. Virol.* **79,** 441–449
14. Paulsen, S. J., Rosenkilde, M. M., Eugen-Olsen, J., and Kledal, T. N. (2005) *J. Virol.* **79,** 536–546
15. Rosenkilde, M. M., and Kledal, T. N. (2006) *Curr. Drug Targets* **7,** 103–118
16. Britt, W. J., and Alford, C. A. (1996) in *Fields Virology* (Fields, B. N., Knipe, D. M., and Howley, P. M., eds) pp. 771–778, Lippincott-Raven, New York
17. Bais, C., Santomasso, B., Coso, O., Arvanitakis, L., Raaka, E. G., Gutkind, J. S., Asch, A. S., Cesarman, E., Gershengorn, M. C., Mesri, E. A., and Gerhengorn, M. C. (1998) *Nature* **391,** 86–89
18. Yang, T. Y., Chen, S. C., Leach, M. W., Manfra, D., Homey, B., Wiekowski, M., Sullivan, L., Jenh, C. H., Narula, S. K., Chensue, S. W., and Lira, S. A. (2000) *J. Exp. Med.* **191,** 445–454
19. Holst, P. J., Rosenkilde, M. M., Manfra, D., Chen, S. C., Wiekowski, M. T., Holst, B., Cifire, F., Lipp, M., Schwartz, T. W., and Lira, S. A. (2001) *J. Clin. Invest.* **108,** 1789–1796
20. Maussang, D., Verzijl, D., van Walsum, M., Leurs, R., Holl, J., Pleskoff, O., Michel, D., van Dongen, G. A., and Smit, M. J. (2006) *Proc. Natl. Acad. Sci. U.S.A.* **103,** 13068–13073
21. Lyngaa, R., Nørregaard, K., Kristensen, M., Kubale, V., Rosenkilde, M. M., and Kledal, T. N. (2010) *Oncogene* **29,** 4388–4398
22. Young, L. S., and Rickinson, A. B. (2004) *Nat. Rev. Cancer* **4,** 757–768
23. Craig, F. E., Johnson, L. R., Harvey, S. A., Nalesnik, M. A., Luo, J. H., Bhattacharya, S. D., and Swerdlow, S. H. (2007) *Diagn. Mol. Pathol.* **16,** 158–168
24. Kostenis, E. (2002) *J. Recept. Signal. Transduct. Res.* **22,** 267–281
25. Benned-Jensen, T., and Rosenkilde, M. M. (2010) *Br. J. Pharmacol.* **159,** 1092–1105
26. Fraile-Ramos, A., Kledal, T. N., Pelchen-Matthews, A., Bowers, K., Schwartz, T. W., and Marsh, M. (2001) *Mol. Biol. Cell* **12,** 1737–1749
27. Elling, C. E., Frimurer, T. M., Gerlach, L. O., Jorgensen, R., Holst, B., and Schwartz, T. W. (2006) *J. Biol. Chem.* **281,** 17337–17346
28. Nygaard, R., Frimurer, T. M., Holst, B., Rosenkilde, M. M., and Schwartz, T. W. (2009) *Trends Pharmacol. Sci.* **30,** 249–259
29. Schwartz, T. W., Frimurer, T. M., Holst, B., Rosenkilde, M. M., and Elling, C. E. (2006) *Annu. Rev. Pharmacol. Toxicol.* **46,** 481–519
30. Strader, C. D., Sigal, I. S., Register, R. B., Candelore, M. R., Rands, E., and Dixon, R. A. (1987) *Proc. Natl. Acad. Sci. U.S.A.* **84,** 4384–4388
31. Jensen, P. C., Nygaard, R., Thiele, S., Elder, A., Zhu, G., Kolbeck, R., Ghosh, S., Schwartz, T. W., and Rosenkilde, M. M. (2007) *Mol. Pharmacol.* **72,** 327–340
32. Trott, O., and Olson, A. J. (2010) *J. Comput. Chem.* **31,** 455–461
33. De Lean, A., Stadel, J. M., and Lefkowitz, R. J. (1980) *J. Biol. Chem.* **255,** 7108–7117
34. Rajagopal, S., Rajagopal, K., and Lefkowitz, R. J. (2010) *Nat. Rev. Drug Discov.* **9,** 373–386
35. Walters, R. W., Shukla, A. K., Kovacs, J. J., Violin, J. D., DeWire, S. M., Lam, C. M., Chen, J. R., Muehlbauer, M. J., Whalen, E. J., and Lefkowitz, R. J. (2009) *J. Clin. Invest.* **119,** 1312–1321
36. McCune, D. F., Edelmann, S. E., Olges, J. R., Post, G. R., Waldrop, B. A., Waugh, D. J., Perez, D. M., and Piascik, M. T. (2000) *Mol. Pharmacol.* **57,** 659–666
37. Azzi, M., Charest, P. G., Angers, S., Rousseau, G., Kohout, T., Bouvier, M., and Piñeyro, G. (2003) *Proc. Natl. Acad. Sci. U.S.A.* **100,** 11406–11411
38. Shin, N., Coates, E., Murgolo, N. J., Morse, K. L., Bayne, M., Strader, C. D., and Monsma, F. J., Jr. (2002) *Mol. Pharmacol.* **62,** 38–47
39. Claeysen, S., Joubert, L., Sebben, M., Bockaert, J., and Dumuis, A. (2003) *J. Biol. Chem.* **278,** 699–702
40. Cussac, D., Palmier, C., Finana, F., De Vries, L., Tardif, S., Léger, C., Bernois, S., and Heusler, P. (2009) *J. Pharmacol. Exp. Ther.* **331,** 222–233
41. Buck, E., and Wells, J. A. (2005) *Proc. Natl. Acad. Sci. U.S.A.* **102,** 2719–2724
42. Jensen, P. C., and Rosenkilde, M. M. (2009) *Methods Enzymol.* **461,** 171–190
43. Han, S. J., Hamdan, F. F., Kim, S. K., Jacobson, K. A., Bloodworth, L. M., Li, B., and Wess, J. (2005) *J. Biol. Chem.* **280,** 34849–34858
44. Pereira, J. P., Kelly, L. M., and Cyster, J. G. (2010) *Int. Immunol.* **22,** 413–419
45. Gottschalk, S., Rooney, C. M., and Heslop, H. E. (2005) *Annu. Rev. Med.* **56,** 29–44
46. Cahir-McFarland, E. D., Carter, K., Rosenwald, A., Giltnane, J. M., Henrickson, S. E., Staudt, L. M., and Kieff, E. (2004) *J. Virol.* **78,** 4108–4119